

was collected to give three replicates, each of 12 needles, for each uptake temperature. Immediately following excision, the fresh weight was measured, and the cut ends of the needles were placed in sealed test tubes with 5 mm of water. These tubes were placed in water baths at selected uptake temperatures. Water uptake at the different temperatures was observed and the percentage of change of the initial fresh weight was plotted against the time during which the change occurred.

The results of the first experiment, run at 8°, 20°, and 37°C, are shown in Fig. 1; each point represents the mean value of the three replicates.

These results suggest that the neglect of a temperature change of 17°C in a standard (20°C) relative turgidity determination leads to an error of only 8 percent, a seemingly trivial error when referred to the 0 to 100 percent scale. However, it is more realistic to gauge the importance of the error by reference to the small range of values of r between full turgor and wilting—the range over which growth and transpiration rates fall from high to very low values. Measurements by Johnston (8) indicate that pine needles wilt at a relative turgidity of about 80 percent. Thus, the 8 percent error in the full range is equivalent to a 40 percent error in the range of r that is of most interest.

The arbitrary basis for the use of an uptake temperature of 20°C was demonstrated further (Fig. 2). In this experiment a tree was held at a temperature of 35°C for 14 hours before sampling, and uptake temperatures of 20° and 35°C were used. Other work indicates that even larger errors may occur with higher temperatures and with other species (7) and conditions.

The size of the temperature effect varies (Figs. 3 and 4, droughted trees). Whereas the first phase of uptake (5) at 20°C is about the same in each experiment, the uptake at 35°C differs considerably. The reason for such marked variability has not been investigated. It is clear that a difference between uptake and *in situ* temperatures often has a large effect on the uptake of water and consequently also on the relative turgidity. This problem is probably of most concern in studies in which the diurnal course of plant water status is to be followed and when there is a large change in leaf temperature during the day.

In practice, the error could be minimized by use of several water baths or

incubators held at different temperatures so as to cover the range of *in situ* leaf temperatures encountered. The w_t determinations could then be made in the bath or incubator at a temperature nearest that of the measured *in situ* leaf temperature.

Measurements of ψ and other water stress indices are also customarily run at a standard temperature. Thus, these measurements are probably subject to error due to the neglect of the temperature effect. Direct proof of this and an elucidation of the mode of action of the temperature effect have been delayed by difficulties encountered here and by others (9) in the development of adequate methods for measuring ψ .

B. D. MILLAR

Division of Plant Industry,
Commonwealth Scientific and Industrial
Research Organization,
Canberra, A.C.T., Australia

References and Notes

1. P. J. Kramer, *Agron. J.* **55**, 31 (1963).
2. H. D. Barrs and P. E. Weatherley, *Australian J. Biol. Sci.* **15**, 413 (1962).
3. B. D. Millar, *Australian J. Agr. Res.* **15**, 85 (1964).

4. P. E. Weatherley and R. O. Slatyer, *Nature* **179**, 1085 (1957).
 5. The uptake of water by excised leaf tissue consists of an initial rapid phase, followed by a slower steady uptake lasting as long as the tissue remains healthy. It is generally accepted that the slower uptake is due to growth of the tissue. There is, however, some controversy about the initial uptake. Barrs and Weatherley (2) suggest that it is due to the initial water deficit alone (that is, a result of the difference in water potential between the tissue and pure free water), and that uptake due to growth commences only after the conclusion of the initial phase. This implies that growth, with its associated uptake of water, cannot commence until the tissue is fully turgid. However, as leaf tissue generally grows at somewhat less than full turgor, this supposition appears to be unrealistic. Yemm and Willis (10) assume that growth uptake is steady throughout. By extrapolating the linear portion (second phase) of the curve back to zero time, the intercept obtained leads to the value of w_t . This is the procedure adopted here.
 6. W. R. Gardner and C. F. Ehlig, *Plant Physiol.* **40**, 705 (1965).
 7. H. O. Werner, *Res. Bull. Nebr. Agr. Exp. Sta.* **176** (1954).
 8. R. D. Johnston, *Australian J. Bot.* **12**, 111 (1964).
 9. S. L. Rawlins, *Science* **146**, 644 (1964); J. E. Box, Jr., *Agron. J.* **57**, 367 (1965); J. R. Lambert and J. van Schilfhaarde, *Soil Sci.* **100**, 1 (1965).
 10. E. W. Yemm and A. J. Willis, *New Phytol.* **53**, 373 (1954).
 11. I thank Mr. G. A. McIntyre of the Division of Mathematical Statistics, CSIRO, for statistical advice.
- 19 July 1966

Ferrosilite III: A Triclinic Pyroxenoid-Type Polymorph of Ferrous Metasilicate

Abstract. *The relationships between the triclinic unit cell of ferrosilite III and those of pyroxmangite, rhodonite, and wollastonite lead to the hypothesis that this polymorph of ferrous metasilicate has a pyroxenoid-type crystal structure with single silicate chains that repeat after every nine silicon tetrahedra. Vector relations between the triclinic cell and an apparent pseudomonoclinic cell support this hypothesis. Although the proposed silicate chain has a longer repeat length than any now known, it represents a logical extension of those found in other pyroxenoids and suggests that even longer repeat lengths may yet be found among phases with pyroxene compositions.*

Ferrosilite, the iron analog of the common pyroxene enstatite (MgSiO_3), does not exist in nature; but two polymorphs having the ferrous metasilicate (FeSiO_3) composition have been synthesized at high temperatures and pressures by Lindsley *et al.* (1) and Akimoto *et al.* (2). These workers have investigated the stability relations of the monoclinic form and the higher temperature orthorhombic form (3, 4), and x-ray data suggest that these polymorphs are isostructural with clinoenstatite and orthoenstatite, respectively (5).

In several experiments made in the low-pressure region of what is thought to be the protoferrosilite stability field (3), the phase present after quenching could not be identified by its powder diffraction pattern. Precession photo-

graphs of single crystals of this material, termed ferrosilite III, showed that it possesses triclinic symmetry but that it exhibits a pseudomonoclinic unit cell similar in size to that of diopside ($\text{CaMgSi}_2\text{O}_6$). According to Lindsley, the stability field of ferrosilite III has not been determined; although the synthesis is reproducible in his apparatus, he believes that this phase forms during the quench. The single-crystal x-ray photographs described in this report are also reproducible; five crystals from different experiments have been examined, all of which yield the same diffraction patterns.

The crudely prismatic shape of several single crystals made it relatively easy to orient them on the precession camera, but in almost all cases the first

Table 1. Comparison of pyroxenoid unit-cell dimensions.

Axis	Angle	Ferrosilite III*	Pyroxmangite (15)	Rhodonite (16)*
<i>a</i>		6.6338 ± 0.0006 Å	6.67 Å	6.7073 ± 0.0004 Å
<i>b</i>		7.4717 ± .0009 Å	7.56 Å	7.6816 ± .0002 Å
<i>c</i>		22.610 ± .002 Å	17.45 Å	12.2337 ± .0004 Å
	α	115.294° ± .006°	113.7°	111.538° ± .002°
	β	80.649° ± .005°	84.0°	85.247° ± .005°
	γ	95.423° ± .006°	94.3°	93.948° ± .005°

* Least-squares refinement of precision-Weissenberg film data.

photographs were identical with that shown in Fig. 1. This pattern is similar to that obtained by precessing about the *b* axis of diopside, except for several weak spots with *l* odd that violate the *c* glide in the diopside space group, *C2/c*. The assumption that ferrosilite III is monoclinic fails as soon as one attempts to take an *a*-axis precession photograph.

Subsequent systematic investigations with the precession camera revealed a very short reciprocal translation, shown in Fig. 2 as parallel to *c** of the triclinic unit cell. After a crystal was re-oriented so that it could be rotated about this direction, the pattern shown in Fig. 2 was obtained. Two other reciprocal-cell translations were selected by referring to photographs of one crystal that exhibited a pronounced prismatic cleavage. The resulting unit cell bears a very close relationship to that of pyroxmangite, one of the triclinic metasilicates, or pyroxenoids (Table 1). The only major difference is that the *c* axis of ferrosilite III is longer

than that of pyroxmangite by 5.16 Å. Viewed in context with metasilicate crystal chemistry, this difference provides the basis for the ferrosilite III structure proposed below.

The known crystal structures of pyroxenes and pyroxenoids may be characterized in terms of approximate closest packing of oxygen atoms, with Si filling tetrahedral interstices and larger cations (Ca, Mn, Mg, Fe, and so forth) occupying octahedral sites (6). Although in all these structures the SiO₄⁻⁴ coordination tetrahedra each share two vertices to form continuous single chains, an essential difference between pyroxenes and the various pyroxenoids is the length of the repeat unit along the silicate chains: in pyroxenes the chain repeats after every two tetrahedra (*Zweierketten*); in wollastonite (CaSiO₃) and bustamite (CaMnSi₂O₆), after every three (*Dreierketten*); in rhodonite ([Mn, Ca]SiO₃), after every five (*Fünferketten*); and in pyroxmangite ([Mn, Fe, Ca, Mg]SiO₃), after every seven (*Siebenerketten*).

Unit cells of pyroxenes are selected so that their *c* axes parallel the silicate chains. The triclinic pyroxenoid unit cells may be selected in the same way, in which case the *c*-axis length is directly related to the number of tetrahedra in the chain repeat unit (7). Since the difference between the *c* axes of ferrosilite III and pyroxmangite is 5.16 Å, or approximately the length of the two-tetrahedra repeat in pyroxene chains, it appears evident that ferrosilite III is also a pyroxenoid, but with a chain repeat of nine silicon tetrahedra, or a *Neuner-kette*. This configuration is compared schematically with those of pyroxenes (represented by diopside), pyroxmangite, rhodonite, and wollastonite in Fig. 3 [modified from a diagram given previously by Prewitt and Peacor (6)]. The structures are viewed normal to the close-packed oxygen layers to emphasize the relationship between the silicate chains.

Although unit-cell relationships alone are a strong indication that a *Neuner-ketten* configuration for ferrosilite III is very likely, further analysis of preliminary x-ray data provides additional support for the model. Because there is a precession direction in ferrosilite III that yields an x-ray pattern similar to that of diopside precessed about its *b* axis (Fig. 1), the ferrosilite III structure projected onto a plane normal to this unidentified axis must be similar to that of diopside projected onto a plane normal to *b*, or (010). The diopside *b* axis

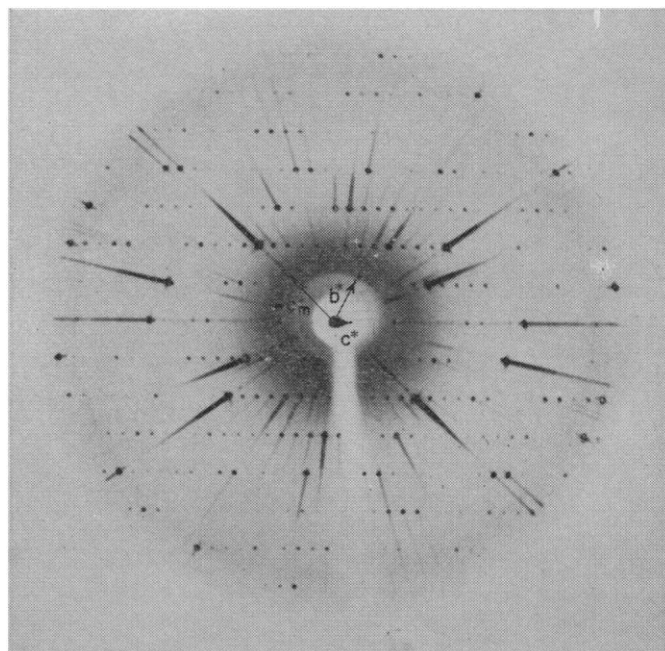
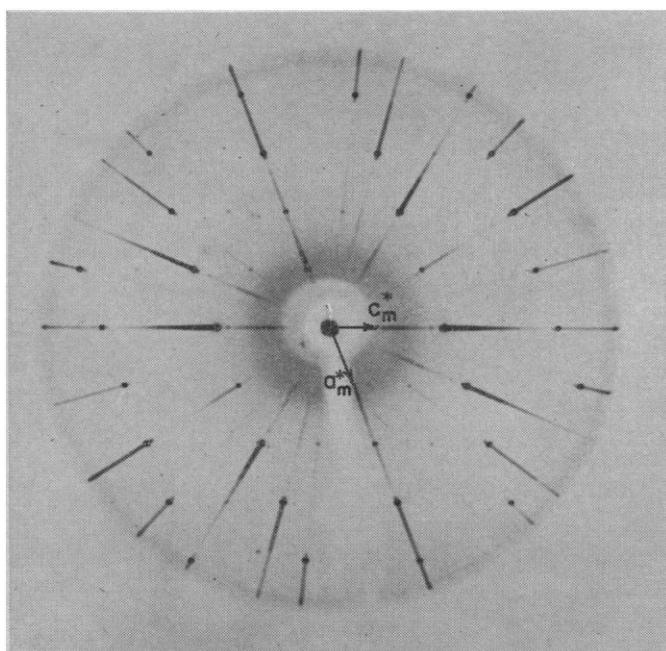


Fig. 1 (left). Precession photograph of ferrosilite III taken about the axis *p* (see text), showing the diopside-like pseudomonoclinic substructure. MoK α , $\mu = 20^\circ$, 67 hours; the *c**_m and *a**_m axes are indicated. Fig. 2 (right). An *a*-axis 0-level precession photograph of ferrosilite III, MoK α , $\mu = 20^\circ$, 40 hours; *b**, *c**, and the pseudomonoclinic *c**_m axes are indicated.

bears two important relationships to the structure (8): (i) it lies in the close-packed oxygen plane (100), and (ii) it is normal to the direction of the silicate chain [001]. Hence the critical question is: Does the corresponding precession direction in ferrosilite III bear similar relationships to a *Neunerketten* model?

To clarify the requirements of relationship ii, observe that the pyroxenoid chains differ from the diopside chain only by "horizontal offsets" after every n tetrahedra, where n is the total repeat number (Fig. 3). Within each unit of n tetrahedra, the direction of the chain is the same as that of diopside. As n increases, the angle ϵ between the chain direction, c , and the direction of the diopside-like units decreases. When $n = \infty$ and there are no offsets, ϵ is zero and the pyroxene chain obtains. Thus relationship ii implies that the precession direction in question should be normal to the direction of the diopside-like portion of the *Neunerketten* chain—not to the ferrosilite III c axis.

In terms of the ferrosilite III unit cell, the precession direction is normal to the pseudomonoclinic $a_m^* - c_m^*$ reciprocal net, Fig. 1. Let a vector parallel to this direction be termed \mathbf{p} ; then $\mathbf{p} = \mathbf{c}_m^* \times \mathbf{a}_m^*$. Inspection of Fig. 2 shows that $\mathbf{c}_m^* = -\mathbf{b}^* + 4\mathbf{c}^*$. The precession pattern of Fig. 1 is obtained by rotating the crystal 48.25° about \mathbf{c}_m^* from the position of Fig. 2; a plot of these relations shows that $\mathbf{a}_m^* = \frac{1}{2}\mathbf{a}^* - \frac{1}{2}\mathbf{b}^*$. Evaluation of the cross-product leads to

$$\mathbf{p} = 2\mathbf{a} - 2\mathbf{b} - \frac{1}{2}\mathbf{c} \quad (1)$$

The close-packed oxygen plane of rhodonite, referred to the Liebau (non-reduced) cell, is parallel to (110) (9). If ferrosilite III bears the inferred close similarity to rhodonite, its close-packed oxygen plane will also be parallel to (110). Thus the condition that \mathbf{p} lie in the close-packed plane will be met if $\mathbf{p} \cdot [110]^* = 0$. Substitution from Eq. 1 and direct evaluation of the dot product gives the anticipated result.

The angular relationships between \mathbf{p} , \mathbf{c} , and the direction of the diopside-like portion of the silicate chain are easily obtained, since the three vectors lie in a plane parallel to (110), the plane of projection of Fig. 3. These relationships are shown schematically in Fig. 4. The angle, δ , between \mathbf{p} and \mathbf{c} , is determined by

$$\delta = \cos^{-1} \left(\frac{\mathbf{p} \cdot \mathbf{c}}{|\mathbf{p}| |\mathbf{c}|} \right) \quad (2)$$

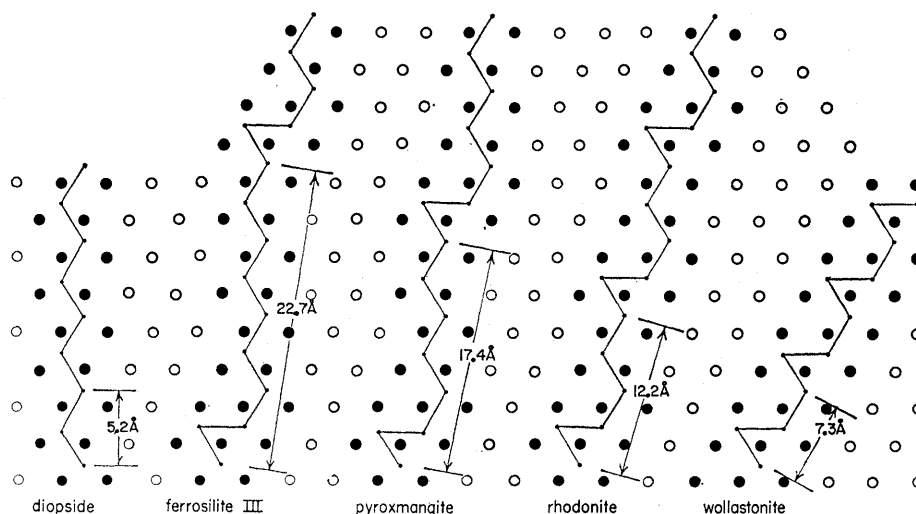


Fig. 3. Schematic diagram of silicate chains and octahedral cation distribution in pyroxenoids and the pyroxene diopside. Solid circles indicate occupied octahedral sites, and lines connect Si atoms in the single chains. The c axes, whose lengths are indicated, are parallel to the chain directions in all cases.

to be 98.2° . In the rhodonite diagram, $+ [110]^*$, the positive normal to the plane of projection, is 90° counterclockwise from $+\mathbf{c}$. Assuming this relationship also holds in ferrosilite III, the positive direction of \mathbf{p} must be counterclockwise 98.2° from $+\mathbf{c}$, since $\mathbf{c} \times \mathbf{p}$ is parallel to $+ [110]^*$. Coupled with the chain configuration of Fig. 3, this directional relationship between $+\mathbf{p}$ and $+\mathbf{c}$ requires a vector parallel to the diopside-like portion of the chain to lie within the angle δ . Thus, the angle between \mathbf{p} and the diopside-like portion of the chain is $\delta - \epsilon$, where ϵ is the acute angle between \mathbf{c} and the diopside-like portion of the chain (see Fig. 4).

An estimate of ϵ can be made from cell geometry and structural considerations as follows: Two sides of an acute triangle enclosing ϵ are c , whose length is 22.61 \AA , and the diopside-like portion of the chain, whose approximate length is four times the diopside c axis (5.25 \AA), or 21 \AA (10). The side opposite ϵ is the chain offset distance, equal to the Si—Si separation, which in all pyroxenes whose structures are well determined is close to 3.05 \AA (11). Based on these estimates $\epsilon = 6.8^\circ$, and $\delta - \epsilon = 91.4^\circ$. If the value of c_m measured from the b_m precession photograph (Fig. 1) is used instead of that for the diopside c axis, the length of the diopside-like portion of the chain becomes $4 \times 5.61 \text{ \AA}$ or 22.44 \AA , ϵ increases to 7.8° , and $\delta - \epsilon$ becomes 90.4° .

This analysis demonstrates that the precession direction of Fig. 1 does indeed correspond to the direction ex-

pected from the model, and supports the proposed *Neunerketten* tetrahedral configuration for ferrosilite III. Qualitative agreement between the expected value of ϵ based on an idealized model and that obtained from x-ray measurements provides additional evidence that the chains are essentially similar to those in diopside and other pyroxenes, except that "offsets" occur after every ninth tetrahedron instead of every seventh in pyroxmangite, every fifth in rhodonite, or every third in wollastonite. A detailed structure analysis is now under way to confirm the proposed structure and to determine the details of the Si and Fe coordination polyhedra.

Liebau (12) has noted a general correlation between octahedral cation size and the frequency of offsets in the silicate chain. As the cation size increases, the chain type proceeds from *Zweierketten*, with no offsets, through *Siebenerketten*, *Fünferketten*, to *Dreierketten*. Ferrosilite III fits this scheme: The pure Fe octahedra must be larger

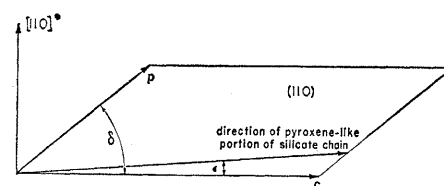


Fig. 4. Schematic diagram of the vector relationships in the (110) plane of pyroxenoids. The angle, ϵ , decreases as the frequency of silicate-chain offsets decreases; δ is determined from x-ray data; and $(\delta - \epsilon)$ is, in ferrosilite III, very close to 90° . The vector, \mathbf{p} , is parallel to the precession direction of Fig. 1.

than those of the Mg-containing pyroxenes but smaller than those in pyroxmangite, which are a mixture of Mn, Fe, Ca, and Mg.

A *Neunerketten* silicate chain in ferrosilite III suggests the possibility of larger repeat units as octahedral cation size decreases. Pigeonites and even enstatite are likely candidates. Recently Perrotta and Stephenson (13) reported the existence of a triclinic enstatite phase (termed "high clinoenstatite") which is apparently stable in the temperature range previously attributed to protoenstatite. This phase, whose stability field is enlarged by the presence of some Ca, may possibly contain pyroxenoid-type silicate chains with repeat units larger than nine. If this is true, the correct unit cell will be very difficult to determine by powder diffraction techniques because ϵ , the angle between c and c_m , decreases (to about 4° to 5° for a 15-unit chain) as the repeat unit increases.

As chain offsets become less frequent they may occur less regularly, leading to the concept of a "disordered" chain. Perhaps, in addition to irregular stacking of octahedral and tetrahedral layers, the "disordered enstatites" reported by Brown and Smith (14) contain irregular chains. Although ferrosilite III would be classified as a pyroxenoid on the basis of the proposed structure, the existence of phases containing longer chain repeat units, or even the postulated variable repeat units, will render the structural distinction between pyroxenes and pyroxenoids obsolete.

CHARLES W. BURNHAM*

*Geophysical Laboratory,
Carnegie Institution of Washington,
Washington, D.C.*

References and Notes

1. D. H. Lindsley, B. T. C. Davis, I. D. MacGregor, *Science* **144**, 73 (1964).
2. S. Akimoto, M. Fujisawa, T. Katsura, *Proc. Japan Acad.* **40**, 272 (1964).
3. D. H. Lindsley, *Carnegie Inst. Wash. Year Book* **64**, 148 (1965).
4. S. Akimoto, T. Katsura, Y. Syono, M. Fujisawa, E. Komada, *Tech. Rept. ISSP, Ser. A, No. 157* (Inst. for Solid State Physics, Univ. of Tokyo, Tokyo, 1964).
5. C. W. Burnham, *Carnegie Inst. Wash. Year Book* **64**, 202 (1965).
6. C. T. Prewitt and D. R. Peacor, *Am. Mineralogist* **49**, 1527 (1964).
7. Although these cells are not the reduced cells reported in the structure determinations of rhodonite (16), bustamite [D. R. Peacor and M. J. Buerger, *Z. Krist.* **117**, 331 (1962)], and wollastonite [M. J. Buerger and C. T. Prewitt, *Proc. Natl. Acad. Sci. U.S.A.* **47**, 1883 (1961)], the parallelism of their c axes to the silicate chains makes them more convenient for structural comparisons.
8. B. E. Warren and W. L. Bragg, *Z. Krist.* **69**, 168 (1928).
9. D. R. Peacor, personal communication.
10. S. P. Clark, Jr., J. F. Schairer, J. de Neuf-

- ville, *Carnegie Inst. Wash. Year Book* **61**, 59 (1962).
11. C. T. Prewitt and C. W. Burnham, *Am. Mineralogist* **51**, 956 (1966).
 12. F. Liebau, *Z. Phys. Chem.* **206**, 73 (1956).
 13. A. J. Perrotta and D. A. Stephenson, *Science* **148**, 1090 (1965).
 14. W. L. Brown and J. V. Smith, *Z. Krist.* **118**, 186 (1963).
 15. F. Liebau, *Acta Cryst.* **12**, 177 (1959).
 16. D. R. Peacor and N. Niizeki, *Z. Krist.* **119**, 98 (1963).
 17. I thank D. H. Lindsley for providing single crystals of ferrosilite III, and for many helpful discussions concerning the synthesis and phase relations of the $FeSiO_3$ polymorphs, and C. T. Prewitt for numerous valuable discussions on pyroxenoid crystal chemistry. D. R. Peacor and C. T. Prewitt reviewed the manuscript.

* Present address: Hoffman Laboratory, Harvard University, Cambridge, Mass. 02138.

2 June 1966

Reaggregation of Insect Cells as Studied by a New Method of Tissue and Organ Culture

Abstract. Cells of the dissociated pupal fat of saturniid moths reaggregated when maintained in vitro in a new type of chamber that permits the culture to "respire" through a film of polyethylene. The fat-body cells are mutually cohesive, but depend on ameoboid hemocytes to bring them together. The hemocytes are also capable of causing the reaggregation of particles of diethylaminoethyl-Sephadex.

In the course of experiments performed for other purposes, we have discovered an improved technique for culture of insect tissues and organs in vitro. The same experiments revealed a phenomenon well known to students of vertebrate embryology but, as far as we are aware, not previously demonstrated in the postembryonic development of organisms higher than sponges—namely, the reaggregation in vitro of dissociated cells to form a discrete tissue. The experiments in question were carried out as follows.

Through a scalpel incision in the facial region, blood was expressed from a pupa of the silkworms *Antheraea polyphemus* or *Hyalophora cecropia* on about the 5th day of adult development. The expressed blood, as is always the case during early adult development, contained great numbers of individual cells of the fat body, which, at this particular phase of the life history, are subject to dissociation by the slightest mechanical disturbance.

Immediately after collecting the blood, we added to it crystals of streptomycin sulfate and phenylthiourea, a potent inhibitor of tyrosinase. Drops of

blood were transferred into the depression of a culture chamber formed by cementing a Lucite plastic washer (19 mm outside diameter, 13 mm inside diameter, 1.0 mm thick) onto a thin (0.05 mm) disc of polyethylene. The blood-filled depression was then capped by placing a glass microscope slide across the washer and sealing it in place with melted wax. The result was a bubble-free, optically flat preparation. Polyethylene, rather than a glass cover slip, was used because of its paradoxical permeability to oxygen and carbon dioxide and impermeability to water or water vapor (1). It occurred to us that the polyethylene film might constitute a lung-like surface and permit the culture to "breathe" by the diffusion of respiratory gases.

In cultures of this type we were amazed to witness the rapid reassembly of the individual fat-body cells into large aggregates. Within an hour or two, the process was conspicuous; in less than a day, virtually all of the cells had reaggregated into a number of large masses (Figs. 1 and 2).

No reaggregation took place when the polyethylene film was covered or replaced by a glass cover slip which was sealed in place with melted wax. The importance of the availability of oxygen was further demonstrated by placing freshly prepared "polyethylene cultures" in an atmosphere of carbon dioxide or nitrogen. Reaggregation was blocked, but was promptly restored when the cultures were returned to air. Reaggregation was also prevented when a crystal of 2,4-dinitrophenol was added to the culture, thereby indicating the importance of the contemporaneous formation of adenosine triphosphate.

The reaggregation of the fat-body cells was reminiscent of the self-reconstruction of dissociated tissues prepared from vertebrate embryos (2). The important difference in this case was that the fat-body cells show no intrinsic motility or locomotion. Under phase-contrast optics one could see that the fat-body cells were being drawn together and reassembled into aggregates by a totally different cell, the ameoboid "plasmatocyte" (3), a type of hemocyte present in the blood in great numbers. This conclusion was confirmed by time-lapse cinematography in which the plasmatocytes were seen to crawl around, frequently adopting a spindle shape with their processes adhering to two or more fat-body cells or groups of cells which were then dragged together